Solar-Terrestrial Physics. 2023. Vol. 9. Iss. 2. P. 31–36. DOI: 10.12737/stp-92202304. © 2023
B. Namuun, B. Tsegmed, L.Y. Li, G.M. Leghari. Published by INFRA-M Academic Publishing House

UDC 533.951, 537.868
DOI: 10.12737/stp-92202304

Received November 22, 2022
Accepted February 21, 2023

DIFFERENCES IN THE RESPONSE TO CME AND CIR DRIVERS OF GEOMAGNETIC DISTURBANCES

B. Namuun
School of Space and Environment, Beihang University, Beijing, China
Institute of Astronomy and Geophysics, Mongolian Academy of Sciences (IAG MAS), Ulaanbaatar, Mongolia

B. Tsegmed
Institute of Astronomy and Geophysics, Mongolian Academy of Sciences (IAG MAS), Ulaanbaatar, Mongolia, tseg@iag.ac.mn

L.Y. Li
School of Space and Environment, Beihang University, Beijing, China
Key Laboratory of Space Environment monitoring and Information Processing of MIIT, Beijing, China

G.M. Leghari
School of Space and Environment, Beihang University, Beijing, China
Pakistan Space and Upper Atmosphere Research Commission (SUPARCO), Islamabad, Pakistan

Abstract. Utilizing 1-minute resolution data on the geomagnetic indices *SYM-H*, *AE*, solar wind parameters (velocity V_{sw} and density N_p), and *z*-component B_z of the interplanetary magnetic field (IMF) during solar cycles 23 and 24, we have statistically analyzed the correlations between geomagnetic activity (storms and substorms), V_{sw}, N_p, B_z, and energy coupling functions of solar wind and Earth's magnetosphere. For the selected 131 CME-driven storms, *SYM-H* stronger depends on V_{sw} and *B* than other parameters, whereas the selected 161 CIR-driven storms have nearly the same dependence on the solar wind electric field, the rate of open magnetic flux $d\varphi/dt$, and the reconnection electric field E_{KL}. Thus, the solar wind electric field and the dayside magnetic reconnection are likely to have different contributions for storms of the two types. During storms of different types, the substorm intensity *AE* relies mainly on the IMF B_z, rate of open magnetic flux and reconnection electric field.

Keywords: solar wind, coronal mass ejections, corotating interaction regions, geomagnetic storms, magnetospheric substorms, correlations

INTRODUCTION

Coronal mass ejections (CMEs) and corotating interaction regions (CIRs) are two typical drivers of geomagnetic storms and magnetospheric substorms [Tsurutani, Gonzalez, 1997; Gonzalez et al., 1999; Li et al., 2018]. According to different drivers, geomagnetic storms are classified as CME-driven and CIR-driven storms [Richardson et al., 2001; Tsurutani et al., 2006; Borovsky, Denton, 2006; Liemohn et al., 2010; Katus et al., 2015]. Intense storms and substorms can cause serious space weather phenomena such as Earth's radiation belts [Li et al., 2006, 2009, 2017, 2020] and plasma sheet [Cao et al., 2013]. Therefore, the solar activity dependence of geomagnetic storms and substorms and their forecast have been hot topics in space weather [Le et al., 2012; Zhao et al., 2022].

The development of geomagnetic storms is associated with the solar wind energy input into Earth's magnetosphere [Du et al., 2008]. Turner et al. have analyzed 118 CME-driven storms and 91 CIR-driven storms during the period from 1995 to 2004 [Turner et al., 2009]. They suggested that the CIR-driven storms provide more energy for the ionosphere and ring current than the CME-driven storms. Verbanac et al. have investigated the magnetospheric activity caused by CIR/HSS (High Speed Streams) structures during the declining phase of solar cycle (2005–2006), and have found that the combination of solar wind parameters (BV^2 and BV) plays an important role in the energy transfer from the solar wind to the magnetosphere [Verbanac et al., 2011]. Yermolaev et al. shows that the magnitude of the interplanetary magnetic field (IMF) *B* in CIRs and sheaths increases with increasing speed of pistons of both types: HSS and ICME; the piston speed increase results in an increase in geoeffectiveness of both compression regions [Yermolaev et al., 2018]. Alexakis and Mavromichalaki have suggested that the velocity of ICME (Interplanetary CME) structure can be used to predict the generation and intensity of geomagnetic storms [Alexakis, Mavromichalaki, 2019].

During storms of different types, the energy and momentum transfers from the solar wind and IMF to Earth's magnetosphere are still under debate. Moreover, the question of the relationship between geomagnetic storms and magnetospheric substorms has been unanswered so far. To distinguish the contributions of the solar wind density, velocity, and IMF to storms of different types, we have selected 131 CMEs, 161 CIR-driven storms, which occurred during solar cycles 23 and 24, and have analyzed their correlation with geomagnetic indices. In addition, we consider the relationship between geomagnetic activity and solar wind — magnetosphere coupling functions such as the reconnection electric field E_{KL} [Kan, Lee, 1979], the rate of open magnetic flux at the magnetopause $d\varphi/dt$, and the energy function ε.

The goal of this paper is to reveal geomagnetic/ auroral activity dependence not only on the solar wind and IMF parameters, but also on energy coupling functions during the solar activity period under study. Moreover, we try to figure out which factor is more effective for the development of geomagnetic storms.

DATA AND METHOD

The 1-min averaged data on solar wind parameters V_{sw}, N_p, B_z, and the geomagnetic indices *SYM-H* and *AE* have been taken from the OMNI database in CDAWeb [https://omniweb.gsfc.nasa.gov/form/omni_min.html]. *AE* denotes the substorm intensity, whereas the 1-min resolution *SYM-H* is often used to replace the 1-hr resolution *Dst* index to indicate the intensity of storms [Wanliss, Showalter, 2006]. For reference, we have also used the sunspot numbers [https://www.sidc.be/silso/datafiles].

The sunspot numbers during solar cycle 23 (1996–2007) are larger than those during solar cycle 24 (2007–2018). Therefore, the CME-driven storms are more intense during solar cycle 23 than during solar cycle 24 [Alexakis, Mavromichalaki, 2019]. In front of CMEs, IMF, V_{sw}, N_p and temperature T increase suddenly and form a strong interplanetary (IP) shock [Kataoka et al., 2005]. However, IMF, V_{sw}, T, and N_p increase gradually around the stream interface of CIRs [Zhang et al., 2008]. Consequently, the CIR-driven and CME-driven storms have different rate of development.

Figure 1 gives two examples of the CIR-driven storm that occurred on January 11, 2000 and the CME-driven storm that occurred on August 3, 1997. The development phases of the storms are indicated by *SYM-H*. Since the increases in IMF B, V_{sw} from ~360 to ~500 km/s and N_p are gradual, there is no storm sudden commencement (SSC) before the main phase of the CIR-driven storm, and the CIR-driven storm develops slowly into the main phase. Moreover, the CIR-driven storm recovery phase is also long because of IMF quasi-periodic southward turn ($B_z < 0$).

In contrast, the CME-driven storm has a prominent SSC because of the impact of the IP shock with the sudden increase in IMF B, V_{sw}, N_p, and its main and recovery phases are short because of fast southward and northward turn of IMF.

According to different features of storms of two types, we have selected 131 CME- and 161 CIR-driven storms with a minimum $Dst \leq -30$ nT from 1996 to 2017. These storm events were selected from the list compiled by Turner et al. [2009], which covered the period from 1996 to 2004. For the period from 2005 to 2017, we have used the information on SSC taken from [https://www.ngdc.noaa.gov/stp/geomag/geoib.html] and [https://isgi.unistra.fr/events_sc.php], V_{sw}, ring current and *Dst* from [https://omniweb.gsfc.nasa.gov/ow.html]. To identify magnetic storms, we took into account several patterns including the occurrence of SSC preceding the storm, the development of V_{sw}, and the behavior of the *Dst* index.

We have calculated Pearson's linear correlation coefficient *CC* between the *SYM-H*, *AE*, and a single solar wind parameters N_p, V_{sw}, and IMF B_z for all selected storms. Furthermore, we estimated *CC* between the geomagnetic indices and combined solar wind parameters.

The combined solar wind parameters represent the energy coupling relationship between the solar wind and Earth's magnetosphere. The energy coupling functions of the solar wind and magnetosphere are calculated through the following empirical formulas. The Akasofu function correlates not only with magnetic storms but also with individual substorm [Akasofu, 1981]. It is expressed as [Perrault, Akasofu, 1978]:

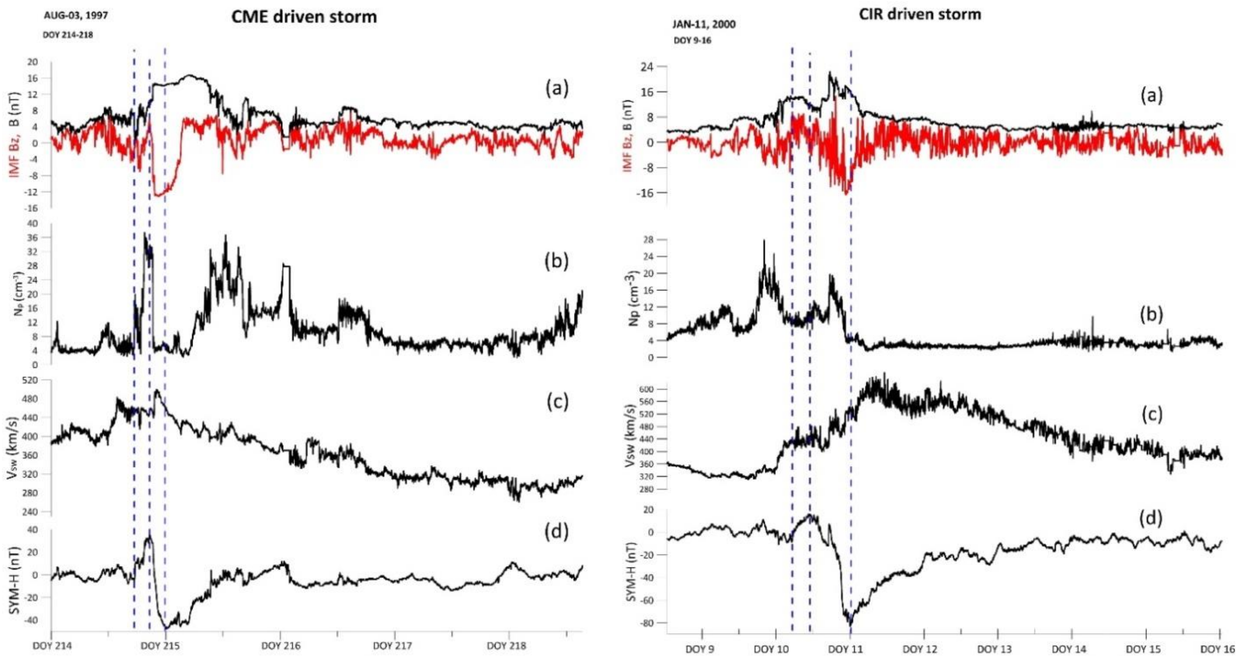

Figure 1. Interplanetary magnetic field and solar wind parameters during CIR-driven and CME-driven storms: IMF B and B_z variations (*a*), N_p (*b*), V_{sw} (*c*), and *SYM-H* (*d*) during CIR/CME-driven storms. Dashed vertical lines indicate the beginning of the initial, main, and recovery phases

$$\varepsilon = V_{sw} B^2 \sin^4(\theta/2) l_0^2, \quad (1)$$

where l_0 is a constant length (~$7R_E$, R_E=6371 km is Earth radius). The scaling factor l_0 was obtained by considering the magnetospheric disturbance phenomena as a manifestation of the dissipation process of energy produced by the solar wind — magnetosphere interaction; θ is the projection of the polar angle of IMF onto YZ plane in solar magnetospheric coordinates, and

$$\theta = \tan^{-1}\left(|B_y|/|B_z|\right), \; B_z > 0, \quad (2)$$

$$\theta = 180° - \tan^{-1}\left(|B_y|/|B_z|\right), B_z < 0. \quad (3)$$

The Akasofu function depends not only on IMF clock angle on YZ plane, but also on $V_{sw}B^2$. $V_{sw}B$ represents the solar wind electric field that plays an essential role in the magnetospheric convection [Burton et al., 1975)].

Moreover, E_{KL} and $d\varphi/dt$ also depend on the solar wind electric field and IMF clock angle. E_{KL} is expressed as [Kan, Lee, 1979]

$$E_{KL} = V_{sw} B \sin^2(\theta/2), \quad (4)$$

$d\varphi/dt$ is expressed as [Newell et al., 2007],

$$\frac{d\varphi}{dt} = V_{sw}{}^{4/3} B^{2/3} \sin^{8/3}(\theta/2), \quad (5)$$

$d\varphi/dt$ is proportional to the rate at which the magnetic flux is opened at the magnetopause, whereas the open magnetic flux depends on E_{KL}. Thus, E_{KL} and $d\varphi/dt$ correlate with the dayside magnetic reconnection that transports solar wind mass, energy, and IMF into the magnetosphere.

STATISTICAL RESULTS

Correlation for CME-driven storms

Figures 2 and 3 display the correlation coefficients *CC* between geomagnetic indices *SYM-H*, *AE*, single solar wind parameter V_{sw}, N_p, IMF B_z, and energy coupling functions during 131 CME-driven storms. Three correlation levels are defined: almost no or weak correlation ($|CC| \leq 0.4$), moderate correlation ($0.4 < |CC| < 0.6$), and strong correlation ($|CC| \geq 0.6$).

The CME-driven storms have a moderate correlation with the solar wind velocity ($CC = -0.51$ between *SYM-H* and V_{sw}) and a strong correlation with the solar wind electric field ($CC = -0.6$ between *SYM-H* and V_{sw}, B). Meanwhile, the CME-driven storms have also a moderate correlation with the open magnetic flux ($CC = -0.5$ between *SYM-H* and $d\varphi/dt$) or the reconnection electric field ($CC = -0.49$ between *SYM-H* and E_{KL}). These results suggest that the CME-driven storms are mainly caused by the convection electric field driven by the high-speed solar wind. Yet, the dependence of the CME-driven storms on N_p and IMF B_z alone is very weak ($CC < 0.4$).

During 131 CME-driven storms, the substorm intensity *AE* has a moderate correlation with IMF B_z ($CC = -0.54$) and strong correlations with the rate of open magnetic flux ($CC = 0.71$ between *SYM-H* and $d\varphi/dt$) and the reconnection electric field (CC= 0.66 between *SYM-H* and E_{KL}), indicating that the substorm activity mainly correlate with the dayside magnetic reconnection.

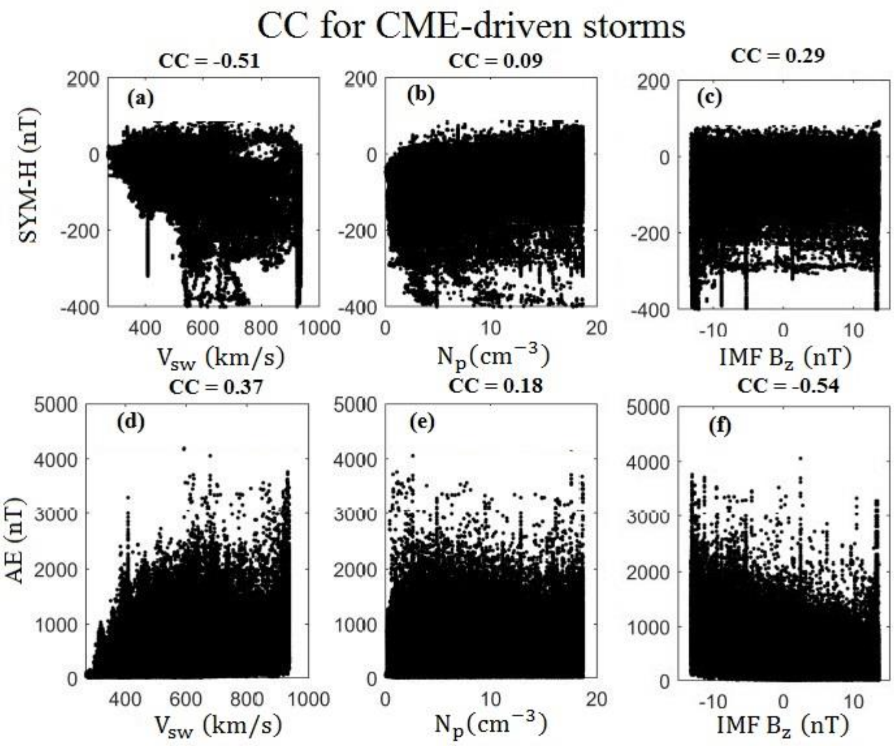

Figure 2. Correlation coefficients *CC* between geomagnetic indices *SYM-H*, *AE*, and single solar wind parameters V_{sw}, N_p, IMF B_z during CME-driven storms

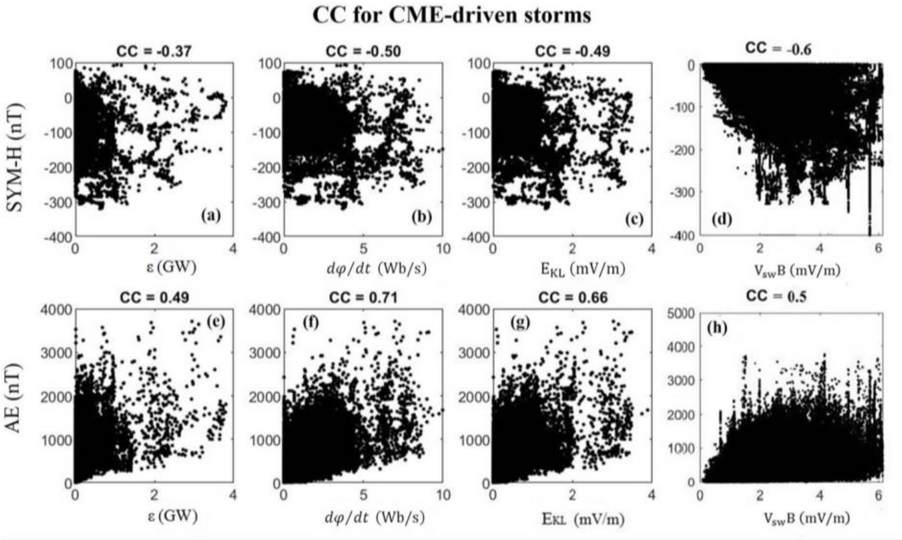

Figure 3. Correlation coefficients *CC* between geomagnetic indices and energy coupling functions during 131 CME-driven storms; ε is the Akasofu function; $d\varphi/dt$ is the rate at which a magnetic flux is opened at the dayside magnetopause; E_{KL} is the reconnection electric field; $V_{sw}B$ is solar wind electric field

However, substorm activities have only a weak correlation with the solar wind velocity (*CC*=0.37 between *AE* and V_{sw}) and moderate correlations with the Akasofu function (*CC*=0.49 between *AE* and ε) and the convection electric field (*CC*=0.5 between *AE* and $V_{sw}B$). Thus, the contribution of the solar wind velocity or the convection electric field is relatively small for the substorm activity.

Correlation for CIR-driven storms

Table lists correlation coefficients *CC* between geomagnetic indices *SYM-H*, *AE*, single solar wind parameters V_{sw}, N_p, IMF B_z, and energy coupling functions for 161 CIR-driven storms and 131 CME-driven storms. The dependence of CIR-driven storms on the solar wind velocity (*CC* = – 0.27) and the convection electric field (*CC* = – 0.48) decreases in comparison with that of the CME-driven storms (*CC*=–0.51 and –0.6), but their dependence on IMF B_z are nearly the same (*CC*=0.29 and 0.28). The dependence of the CIR-driven storms on the convection electric field (*CC*=–0.48 between *SYM-H* and $V_{sw}B$) is comparable to that on the rate of open magnetic flux (*CC*=–0.42 between *SYM-H* and $d\varphi/dt$) and the reconnection electric field (*CC*=–0.44 between *SYM-H* and E_{KL}), indicating that the CIR-driven storms depend simultaneously on the convection electric field and the dayside magnetic reconnection.

During CIR-driven storms, *AE* has a moderate correlation with IMF B_z (*CC* = – 0.56) and strong correlations with the rate of open magnetic flux (*CC* = 0.64 between *AE* and $d\varphi/dt$) and the reconnection electric field (*CC*= 0.64 between *AE* and E_{KL}), indicating that substorm activity is also closely associated with the dayside magnetic reconnection. However, the dependence of the substorm activity on the solar wind velocity and the convection electric field decreases remarkably during CIR-driven storms.

Correlation coefficients for CME and CIR-driven storms

CME-driven storms							
	V_{sw}	N_p	B_z	ε	$d\varphi/dt$	E_{KL}	$V_{sw}B$
SYM-H	– 0.51	0.09	0.29	– 0.37	– 0.50	– 0.49	– 0.6
AE	0.37	0.18	– 0.54	0.49	0.71	0.66	0.5

CIR-driven storms							
	V_{sw}	N_p	B_z	ε	$d\varphi/dt$	E_{KL}	$V_{sw}B$
SYM-H	– 0.27	0.15	0.28	– 0.39	– 0.42	– 0.44	– 0.48
AE	0.08	0.14	– 0.56	0.51	0.64	0.64	0.39

DISCUSSION

The space parameter data and geomagnetic field indices provided on the Internet have different time resolutions such as 1 min, 5-min, and 1 hr. Badruddin et al. [2022] have studied the correlation coefficients of the solar wind parameters and IMF with geomagnetic field indices of 10 selected individual storms, using three time resolutions. The results show that the correlation coefficient between *Dst* (1-hour or smoothed data) and the solar wind parameters turns out to be higher than 0.5 only during the main phase of 50 % of storms. The results also suggest that the hourly development of geomagnetic storms during the main phase could not be unambiguously associated with a simultaneous change in solar wind parameters. High-resolution data may be helpful not only in understanding the physical processes during the development of a geomagnetic storm but also in predicting space weather.

Although there is no obvious correlation between the CME-driven storms and IMF B_z alone (*CC*=0.29), the CME-driven storms have also moderate correlations (*CC* > 0.4) with the rate of open magnetic flux and the reconnection electric field (combined solar wind parameters). The dependence of the CME-driven storms (*CC* = – 0.6) is stronger on the convection electric field than the rate of open magnetic flux and the reconnection electric field (*CC* = – 0.5, – 0.49). Thus, the contribution of the convection electric field to the CME-driven storms is likely to be larger than those of the dayside magnetic reconnection $d\varphi/dt$ and E_{KL}. However, the CIR-driven storms have nearly the same dependence on the three parameters ($CC = -0.42$, -0.44, -0.48), thereby suggesting that the convection electric field and the dayside magnetic reconnection have nearly the same contributions to the development of CIR-driven storms.

During these storms, the substorm intensity relies largely on IMF B_z, the rate of open magnetic flux, and the reconnection electric field. The solar wind velocity or convection electric field contribution is relatively small for substorms. Although magnetospheric substorms mainly occur in the nightside magnetosphere [Baker et al., 1996; Duan et al., 2011] substorm activity can promote the ring current through injections of hot and energetic particles as suggested by previous observations [He et al., 2016]. According to our statistical analysis, we have found a moderate correlation between the substorm intensity (*AE*) and both CME-driven and CIR-driven storms (*SYM-H*), with correlation coefficients of –0.51 and –0.5 respectively. This confirms that both substorms and enhanced convection contribute to enhancement of a storm-time ring current [Lui et al., 2001].

SUMMARY AND CONCLUSIONS

By analyzing the correlation coefficients between geomagnetic indices *SYM-H*, *AE*, single solar wind parameters, and energy coupling functions for 131 CME-driven and 161 CIR-driven storms we have found that the CME-driven storms stronger depend on the solar wind velocity V_{sw} and the convective electric field $V_{sw}B$ than other parameters, whereas the CIR-driven storms have nearly the same dependence on the solar wind electric field, the rate of open magnetic flux $d\varphi/dt$, and the reconnection electric field E_{KL}. The different dependence indicates that the convection electric field driven by high-speed solar wind play a dominant role in the development of the CME-driven storms but the convection electric field contribution to the CIR-driven storms may be comparable to that of the dayside magnetic reconnection.

Interestingly, storms of the two types have moderate dependence on the substorm intensity *AE*, suggesting that substorm activity promotes the enhancement of geomagnetic storms to some extent. This conclusion is in line with the results obtained in [Gonzalez et al., 1994; Boroyev, Vasiliev, 2020]. The substorm intensity relies strongly on IMF B_z, rate of open magnetic flux, and reconnection electric field, but their dependence on the solar wind velocity and the solar wind electric field are relatively weak. This indicates that the dayside magnetic reconnection plays a crucial role in the solar wind energy transfer to Earth's magnetosphere and the energy storage and release in the magnetotail during substorms.

The data sets for this study were obtained from the OMNI database [https://omniweb.gsfc.nasa.gov/form/omni_min.html]. We sincerely acknowledge all teams for the OMNI database. We also thank Center for Space Magnetism, Kyoto University for providing *Dst* index data.

REFERENCES

Akasofu S.I. Energy coupling between the solar wind and the magnetosphere. *Space Sci. Rev*. 1981, vol. 28, pp. 121–190. DOI: 10.1007/BF00218810.

Alexakis P., Mavromichalaki H. Statistical analysis of interplanetary coronal mass ejections and their geoeffectiveness during the solar cycles 23 and 24. *Astrophys Space Sci*. 2019, vol. 364, iss. 11, article id. 187, 14 p. DOI: 10.1007/s10509-019-3677-y.

Badruddin B., Aslam O.P.M., Derouich M. Study of the development of geomagnetic storms in the magnetosphere using solar wind data of three different time resolutions. *Astrophys. Space Sci*. 2022, vol. 367, iss. 1, article id.10. DOI: 10.1007/s10509-021-04030-5.

Baker D.N., Pulkkinen T.I., Angelopoulos V., Baumjohann W., McPherron R.L. Neutral line model of substorms: Past results and present view. *J. Geophys. Res*. 1996, vol. 101, iss. A6, pp. 12975–13010. DOI: 10.1029/95JA03753.

Borovsky J.E., Denton M.H. Differences between CME-driven storms and CIR-driven storms. *J. Geophys. Res*. 2006, vol. 111, iss. A7, CiteID A07S08. DOI: 10.1029/2005JA011447.

Boroyev R.N., Vasiliev M.S. Relationship of the ASY-H index with interplanetary medium parameters and auroral activity in magnetic storm main phases during CIR and ICME events. *Solar-Terr. Phys*. 2020, vol. 6, iss. 1, pp. 35–40. DOI: 10.12737/stp-61202004.

Burton R.K., McPherron R.L., Russell C.T. An empirical relationship between interplanetary conditions and Dst. *J. Geophys. Res*. 1975, vol. 80, iss. 31, p. 4204. DOI: 10.1029/JA080i031p04204.

Cao J., Duan A., Reme H., Dandouras I. Relations of the energetic proton fluxes in the central plasma sheet with solar wind and geomagnetic activities. *J. Geophys. Res.: Space Phys*. 2013, vol. 118, pp. 7226–7236. DOI: 10.1002/2013JA019289.

Du A.M., Tsurutani B.T., Sun W. Anomalous geomagnetic storm of 21–22 January 2005: A storm main phase during northward IMFs. *J. Geophys. Res*. 2008, vol. 113, iss. A10, CiteID A10214. DOI: 10.1029/2008JA013284.

Duan S.P., Liu Z.X., Liang J., Zhang Y., Angelopoulos V. Multiple magnetic dipolarizations observed by THEMIS during a substorm. *Ann. Geophys*. 2011, vol. 29, pp. 331–339. DOI: 10.5194/angeo-29-331-2011.

Gonzalez W.D., Joselyn J.A., Kamide Y., Kroehl H.W., Rostoker G., Tsurutani B.T., et al. What is a geomagnetic storm? *J. Geophys. Res.: Space Phys*. 1994, vol. 99, iss. A4, pp. 5771–5792. DOI: 10.1029/93JA02867.

Gonzalez W.D., Tsurutani B.T., Gonzalez A.L.C. Interplanetary origin of geomagnetic storms. *Space Sci. Rev*. 1999, vol. 88, pp. 529–562. DOI: 10.1023/A:1005160129098

He Z., Dai L., Wang C., Duan S., Zhang L., Chen T., Roth I. Contributions of substorm injections to SYM-H depressions in the main phase of storms. *J. Geophys. Res.: Space Phys*. 2016, vol. 121, pp. 11729–11736. DOI: 10.1002/2016JA023218.

Kan J.R., Lee L.C. Energy coupling function and solar wind-magnetosphere dynamo. *Geophys. Res. Lett*. 1979, vol. 6, iss. 7, pp. 577–580. DOI: 10.1029/GL006i007p00577.

Kataoka R., Watari S., Shimada N., Shimazu H., Marubashi K. Downstream structures of interplanetary fast shocks associated with coronal mass ejections. *Geophys. Res. Lett*. 2005, vol. 32, iss. 12, CiteID L12103. DOI: 10.1029/2005GL022777.

Katus R.M., Liemohn M.W., Ionides E.L., Ilie R., Welling D., Sarno-Smith L.K. Statistical analysis of the geomagnetic response to different solar wind drivers and the dependence on storm intensity. *J. Geophys. Res.: Space Phys*. 2015, vol. 120, pp. 310–327. DOI: 10.1002/2014JA020712.

Le G.M., Cai Z.Y., Wang H.N., Zhu Y.T. Solar cycle distribution of great geomagnetic storms. *Astrophys Space Sci*. 2012, vol. 339, pp. 151–156. DOI: 10.1007/s10509-011-0960-y.

Li L.Y., Wang Z.Q. The effects of solar wind dynamic pressure changes on the substorm auroras and energetic electron injections on 24 August 2005. *J. Geophys. Res.: Space Phys.* 2018, vol. 123, pp. 385–399. DOI: 10.1002/2017JA024628.

Li L.Y., Cao J.B., Zhou G.C. Relation between the variation of geomagnetospheric relativistic electron flux and storm/substorm. Chinese J. Geophys. 2006, vol. 49, pp. 9–15.

Li L.Y., Cao J.B., Zhou G.C., Li X. Statistical roles of storms and substorms in changing the entire outer zone relativistic electron population. *J. Geophys. Res.* 2009, vol. 114, iss. A12, CiteID A12214. DOI: 10.1029/2009JA014333.

Li L.Y., Yu J., Cao J.B., Yang J.Y., Li X, Baker D.N., et al. Roles of whistler mode waves and magnetosonic waves in changing the outer radiation belt and the slot region. *J. Geophys. Res.: Space Phys*. 2017, vol. 122, pp. 5431–5448. DOI: 10.1002/2016JA023634.

Li L.Y., Zhou S.P., Wei S.H., Yang J.Y., Sauvaud J.A., Berthelier J.J. The day-night difference and geomagnetic activity variation of energetic electron fluxes in region of South Atlantic anomaly. *Space Weather*. 2020, vol. 18, iss. 9, e2020SW002479. DOI: 10.1029/2020SW002479.

Liemohn M.W., Jazowski M., Kozyra J.U., Ganushkina N., Thomsen M.F., Borovsky J.E. CIR versus CME drivers of the ring current during intense magnetic storms. *Proc. Royal Society. London, Ser. A*. 2010, vol. 466, pp. 3305–3328. DOI: 10.1098/rspa.2010.0075.

Lui A.T.Y., McEntire R.W., Baker K.B. A new insight on the cause of magnetic storms. *Geophys. Res. Lett*. 2001, vol. 28, pp. 3413–3416. DOI: 10.1029/2001GL013281.

Newell P.T., Sotirelis T., Liou K., Meng C.-I., Rich F.J. A nearly universal solar wind-magnetosphere coupling function inferred from 10 magnetospheric state variables. *J. Geophys. Res.* 2007, vol. 112, iss. A1, CiteID A01206. DOI: 10.1029/2006JA012015.

Perrault P., Akasofu S.I. A study of geomagnetic storms. *Geophys. J. Intern*. 1978, vol. 54, pp. 547–573. DOI: 10.1111/j.1365-246X.1978.tb05494.x.

Richardson I.G., Cliver E.W., Cane H.V. Sources of geomagnetic storms for solar minimum and maximum conditions during 1972–2000. *Geophys Res Lett*. 2001, vol. 28, pp. 2569–2572. DOI: 10.1029/2001GL013052.

Tsurutani B.T., Gonzalez W.D. The interplanetary causes of magnetic storms: a review. *Magnetic Storms*. 1997, vol. 98. p. 77. AGU Press, Washington D.C. DOI: 10.1029/GM098p0077.

Tsurutani B.T., Gonzalez W.D., Gonzalez A.L.C., Guarnieri F.L., Gopalswamy N., Grande M., et al. Corotating solar wind streams and recurrent geomagnetic activity: A review. *J. Geophys. Res.*, 2006, vol. 111, iss. A7, CiteID A07S01. DOI: 10.1029/2005JA011273.

Turner N.E., Cramer W.D., Earles S.K., Emery B.A. Geoefficiency and energy partitioning in CIR-driven and CME-driven storms. *J. Atmosph. Solar-Terr. Phys.* 2009, vol. 71, iss. 10–11, pp. 1023–1031. DOI: 10.1016/j.jastp.2009.02.005.

Verbanac G., Vršnak B., Živković S., Hojsak T., Veronig A.M., Temmer M. Solar wind high-velocity streams and related geomagnetic activity in the declining phase of solar cycle 23. *Astron. Astrophys*. 2011, vol. 533. id. A49, 6 p. DOI: 10.1051/0004-6361/201116615.

Wanliss J.A., Showalter K.M. High-resolution global storm index:Dstversus SYM-H. *J. Geophys. Res.* 2006, vol. 111, iss. A2, CiteID A02202. DOI: 10.1029/2005ja011034.

Yermolaev Yu.I., Lodkina I.G., Nikolaeva N.S., Yermolaev M.Yu., Riazantseva M.O., Rakhmanova L.S. Statistic study of the geoeffectiveness of compression regions CIRs and Sheaths. *J. Atmosph. Solar-Terr. Phys*. 2018, vol. 180, pp. 52–59. DOI: 10.1016/j.jastp.2018.01.027.

Zhang Y., Sun W., Feng X.S., Deehr C.S., Fry C.D., Dryer M. Statistical analysis of corotating interaction regions and their geoeffectiveness during solar cycle 23. *J. Geophys. Res.* 2008, vol. 113, iss. A8, CiteID A08106. DOI: 10.1029/2008JA013095.

Zhao M.X., Le G.M., Lu J.Y. Can we estimate the intensities of great geomagnetic storms (ΔSYM-H $\le$ –200 nT) with the burton equation or the O'Brien and McPherron equation? *Astrophys. J.* 2022, vol. 928, p. 18. DOI: 10.3847/1538-4357/ac50a8.

URL: https://omniweb.gsfc.nasa.gov/form/omni_min.html (accessed April 6, 2023).

URL: https://www.sidc.be/silso/datafiles (accessed April 6, 2023).

URL: https://www.ngdc.noaa.gov/stp/geomag/geoib.html.

URL: https://isgi.unistra.fr/events_sc.php.

Original Russian version: Namuun B., Tsegmed B., Li L.Y., Leghari G.M., published in Solnechno-zemnaya fizika. 2023. Vol. 9. Iss. 2. P. 35–40. DOI: 10.12737/szf-92202304. © 2023 INFRA-M Academic Publishing House (Nauchno-Izdatelskii Tsentr INFRA-M)

How to cite this article

Namuun B., Tsegmed B., Li L.Y., Leghari G.M. Differences in the response to CME and CIR drivers of geomagnetic disturbances. *Solar-Terrestrial Physics*. 2023. Vol. 9. Iss. 2. P. 31–36. DOI: 10.12737/stp-92202304.